CHAPTER - IV

CHAPTER - IV

4 X-RAY K-ABSORPTION SPECTRAL STUDIES OF COPPER SALTS

4.1 Introduction

X-ray Absorption Fine Structure (XAFS) spectroscopy is a unique tool for studying at the atomic and molecular scale and the local structure around selected elements that are contained within a material. XAFS can be applied not only to crystals, but also to materials that possess little or no long-range translational order: amorphous systems, glasses, quasicrystals, disordered films, membranes, solutions, liquids, metalloproteinase even molecular gases. This versatility allows it to be used in a wide variety of disciplines: physics, chemistry, biology, biophysics, medicine, engineering, environmental science, materials science and geology.

This chapter gives the results of the X-ray K-absorption spectral studies carried out on some copper salts, viz, Copper Chloride, Copper Sulphate, Copper Bromide, Copper Acetate and Copper Nitrate. The salts with their Molecular Formulae are given in the table 4.2.

Introduction to Copper metal

Copper is a chemical element with the symbol **Cu** (due to Latin word: *cuprum*) and atomic number is 29. It is a ductile metal with very high thermal and electrical conductivity. Pure copper is rather soft and malleable and a freshly-exposed surface has a pinkish or peachy colour. Gold, caesium and copper are the only metallic elements with a natural colour other than gray or white. It is used as a thermal conductor, an electrical conductor, a building material, and a constituent of various metal alloys. Copper compounds are known in several oxidation states, usually 2+, where they often impart blue or green colours to natural minerals such as turquoise and have been used historically widely as pigments. Copper as both metal and pigmented salt, has a significant presence in decorative art. Copper 2+ ions are soluble in water, where they function at low concentration as bacteriostatic substances

and fungicides. For this reason copper metal can be used as an anti-germ surface that can add to the anti-bacterial and antimicrobial features of buildings such as hospitals.[128]

Properties of Cu salt :-

a) Properties of $CuCl_2.2H_2O$:-

Copper (II) chloride is the chemical compound with the formula $CuCl_2$. This is a yellow-brown solid which slowly absorbs moisture to form a blue-green dihydrate.

Anhydrous $CuCl_2$ adopts a distorted cadmium iodide structure. Most copper(II) compounds exhibit distortions from idealized octahedral geometry due to the Jahn-Teller effect, which in this case describes the localisation of one d-electron into a molecular orbital that is strongly antibonding with respect to a pair of ligands. In $CuCl_2(H_2O)_2$ the copper can be described as a highly distorted octahedral complex, the Cu(II) center being surrounded by two water ligands and four chloride ligands, which bridge asymmetrically to other Cu centers.

Copper (II) chloride dissociates in aqueous solution to give the blue color of $[Cu(H_2O)_6]^{2+}$ and yellow or red color of the halide complexes of the formula $[CuCl_{2+x}]^{x-}$. Concentrated solutions of $CuCl_2$ appear green because of the combination of these various chromophores. The color of the dilute solution depends on temperature, being green around 100 °C and blue at room temperature.

b) Properties of $CuSO_4.5H_2O$:-

Copper (II) sulphate is the chemical compound with the formula $CuSO_4$. This salt exists as a series of compounds that differ in their degree of hydration. The anhydrous form is a pale green or gray-white powder, whereas the pentahydrate, the most commonly encountered salt, is bright blue. The anhydrous form occurs as a rare mineral known as chalcocyanite. The hydrated copper sulphate occurs in nature as chalcanthite(pentahydrate), and two more rare ones: bonattite (trihydrate) and boothite (heptahydrate). Archaic names for copper (II) sulphate are "blue vitriol" and "bluestone".

Since it is available commercially, copper sulfate is usually purchased and not prepared in the laboratory. It can be made by the action of sulphuric acid on a variety

[128] Cullity B.D., Elements of X-ray Diffraction, Second Edition,(1978).

of copper(II) compounds, for example copper(II) oxide; this oxide can be generated with the addition of hydrogen peroxide to the acid. It may also be prepared by electrolyzing sulphuric acid, using copper electrodes.

Copper sulphate pentahydrate decomposes before melting, losing four water molecules at 110 °C and all five at 150 °C. At 650 °C, copper(II) sulphate decomposes into copper(II) oxide (CuO) and sulfur trioxide (SO_3). Its blue color is due to water of hydration. When heated in an open flame the crystals are dehydrated and turn grayish-white.

Copper sulphate pentahydrate is a fungicide. Mixed with lime it is called Bordeaux mixture and used to control fungus on grapes, melons, and other berries. Another application is Cheshunt compound, a mixture of copper sulphate and ammonium carbonate used in horticulture to prevent damping off in seedlings. Its use as an herbicide is not agricultural, but instead for control of invasive exotic aquatic plants and the roots of other invasive plants near various pipes that contain water. A dilute solution of copper sulfate is used to treat aquarium fish for various parasitic infections, and is also used to remove snails from aquariums. However, as the copper ions are also highly toxic to the fish, care must be taken with the dosage. Most species of algae can be controlled with very low concentrations of copper sulphate. Copper sulfate inhibits growth of bacteria such as E. coli.

c) Properties of $CuBr_2$:-

Copper Bromide is generally immediately available in most volumes. High purity, submicron and nanopowder forms may be considered. Metallic Bromides are marketed under the trade name AE Bromides™. Most metal bromide compounds are water soluble for uses in water treatment, chemical analysis and in ultra high purity for certain crystal growth applications. Bromide in an aqueous solution can be detected by adding carbon disulfide (CS2) and chlorine. American Elements produces too many standard grades when applicable, including Mil Spec (military grade); ACS, Reagent and Technical Grade; Food, Agricultural and Pharmaceutical Grade; Optical Grade, USP and EP/BP (European Pharmacopoeia/British Pharmacopoeia) and follows applicable ASTM testing standards. Typical and custom packaging is available. Additional technical, research and safety (MSDS) information is available as is a Reference Calculator for converting relevant units of measurement.

d) Properties of Cu $(CH_3COO)_2.H_2O$:-

Copper (II) acetate, also referred to as cupric acetate, is the chemical compound with the formula $Cu(OAc)_2$ where AcO^- is acetate ($CH_3CO_2^-$). The hydrated derivative, which contains one molecule of water for each Cu atom, is available commercially. $Cu(OAc)_2$ is a dark green crystalline solid, whereas $Cu(OAc)_2(H_2O)_2$ is more bluish-green. Since ancient times, copper acetates of some form have been used as fungicides and green pigments. Today, copper acetate is used as a source of copper(II) in inorganic synthesis and as a catalyst or an oxidizing agent in organic synthesis. Copper acetate, like all copper compounds, emits a blue-green glow in a flame.

e) Properties of Cu $(NO_3)_2.3H_{2O}$

Copper nitrate is in the form of blue crystal, easily to deliquesce. Relative density:2.05 Melting Point: 114.5.Decompose and dissolve in water and ethanol when heats up to 170. Aqueous solution assumes acidity, has oxidizability. It will cause combustion and explosion if heats, rubs, hits with combustible. It will produce poisonous and excitant nitrogen oxides when combusts.

4.2 Experimental

The DEXAFS set-up

The detailed description of the Dispersive Extended X-ray Absorption Fine Structure (DEXAFS) beamline (BL-8) has already been given in chapter-II of this thesis. The beamline is shown in figs. 2.7 to 2.19 and is dedicated to X-ray absorption spectroscopy in the transmission mode, using dispersive optics. In this beamline a bent crystal (Si 111) polychromator is used to select a band of energy from the white synchrotron beam which is horizontally dispersed and focused on the sample. The crystal is bent in the shape of an ellipse in such a way that source & sample positions are at two foci of the ellipse (fig. 2.14). The transmitted beam intensity from the sample is recorded on a position sensitive CCD detector, thus enabling recording of the whole EXAFS spectrum around an absorption edge in a single shot (typical acquisition time of one spectrum is ~300 msec). A mirror is used prior to the polychromator for vertical focusing and higher harmonics rejection. The different parameters of the beamline are given below in table 4.1.

The experimental station of the beamline

The experimental station consists of a θ-2θ goniometer with a telescopic 2θ arm on which sample and detector stages are mounted. The polychromator is mounted on the θ axis. Both θ and 2 θ motions are independently controlled through a PC. The telescopic arm moves on a granite slab with pneumatic air pads. Sample and detector stages are provided with remote controlled X-Y-Z and tilt mechanisms. Sample stage has facility to mount 12 samples (maximum sample dia: 25 mm) at a time; any sample can be brought into the beam path for transmission measurement remotely. Generally samples in pellet or powder form can easily be mounted on the sample holder. Liquid samples confined in a proper cell with X-ray transmission window can also be mounted. A high temperature (up to 750K) cell, which can accommodate sample up to 12 mm dia, is available for temperature dependent EXAFS studies. A low temperature sample environment will also be inducted soon in the beamline. Features of the experimental station of the beamline are summarized below in table 4.1 (a).

Table 4.1 Parameters of DEXAFS beamline (BL-8) at Indus-2

Source	Bending magnet (2.5 GeV Indus-2 Source)
Energy range	5-20 keV
Acceptance	1.5 mrad horizontal x 0.2 mrad vertical
Pre-mirror	Rh coated meridional cylindrical mirror with fixed radius of curvature of 1319m, Horizontally mounted for vertical focusing and higher harmonic rejection
Mo nochromator	Elliptically bent Si(111) Polychromator Vertically mounted on a mechanical bender Mean Radius variable between 2 m to 20 m
Post mirror	Nil
Observed spot size @sample position	250microns(H) x 500microns(V) at 20keV
Observed resolution	5 x 103 @ 20 keV
	7.5 x 103 @13 keV
	8.5 x 103 @ 11 keV
Photon flux	1012 photons/sec/1000eV bandwidth
Typical acquisition time for one EXAFS spectrum	300 msec
Sample environment	Mount available for various forms of samples viz., powder, pellets, liquids etc. High temperature (450º C) reaction cell to study in-situ kinetics for pellet samples

Table 4.1 (a) Features of the experimental station of the beamline	
Angular resolution of goniometer	18 arc sec
2 θ range	-5 to 45 degree
Sample and detector manipulations	X, Y (±15 mm), Z (-10 to 35 mm), tilts (±50)
Sample environment	Air/vacuum
Sample temperature range	300 to 750 K

Calibration of the beamline

On this beamline, before any EXAFS spectrum is recorded, the crystal bender and the goniometer have to be set so as to cover the energy range of the spectra. Then a procedure for energy calibration for that particular setting has to be followed. The various aspects of the calibration and the procedure, and is to be followed at this beamline for EXAFS measurements, has been described in chapter II of this thesis.

The various aspects of the calibration and the procedure, which is recommended by Gaur et al. and is to be followed at this beamline for EXAFS measurements, has been described in chapter II of this thesis. The K-absorption spectra were recorded at the Dispersive Extended X-ray Absorption Fine Structure (DEXAFS) beamline, which has been recently set-up by Applied Spectroscopy Division, BARC at the Indus-2 synchrotron radiation source at Raja Ramanna Centre for Advanced Technology (RRCAT), Indore,[129] which gives very high intensity X-rays. This beamline which is suitable for recording X-ray absorption spectra, called BL-8 dispersive EXAFS beamline. The XAFS data of all the salts were calibrated and analysed using the available computer software packages Athena version 0.8.061[130]. It is well known that the fine structure in the vicinity of an X-ray absorption discontinuity is influenced by the immediate surroundings of the absorbing atom. Studies of the K-edge and the associated fine structure help in understanding the environment of a metal ion in its complexes and biologically important molecules. Chemical shifts as obtained by X-ray absorption spectroscopic studies have yielded

[129] Das N. C., Jha S. N., Bhattacharya D., Poswal A. K., Sinha A. K. and Mishra V. K., 2004, Sadhana, **29**, 5, 545. Bhattacharya D., Poswal A. K., Jha S. N., Sangeeta and Sabharwal S. C., 2009(a), Bull. Mater. Sci., **32**, 1, 103. Bhattacharyya D., Poswal A. K., Jha S. N., Sangeeta and Sabharwal S. C. 2009(b), Nucl. Instrum. Meth. A, **609**, 286

[130] Gaur A Ph. D. theses, Vikram Universty, 2012.

useful information in various kinds of samples having biological relevance and utility in pharmacology.[131]

4.3 Results and Discussion

In an XAFS experiment the incident and transmitted X-ray intensities are measured as a function of energy. The intensity of the x-ray after passing through a sample of thickness x is given by:

$$\mathbf{I_t = I_0 e^{-\mu x}}$$

Where μ is the absorption coefficient and x is the thickness of the absorber, the absorption μ (E) corresponding to the photon energy (E). The plot of absorption versus photon energy is obtained by recording the intensities I0 and It, as the CCD outputs, without and with the sample, respectively, and the absorption coefficient μ is obtained using above relation. When the absorption is plotted as a function of E, the experimental spectra show three features:

(1) A decrease in X-ray absorption with increasing energy in the pre-edge region.
(2) A sharp rise at certain energy called edge.
(3) A series of oscillatory structure that modulate the absorption in the Post - edge region.

The plot of absorption versus photon energy is obtained by recording the intensities I_0 and I_t, as the CCD outputs, without and with the sample, respectively, and the absorption coefficient **μ** is obtained using above relation. The experimental data has been analyzed using the available computer software package Athena version 0.8.061. The various steps of the procedure of the analysis are given in figures 4.1-4.6.

The absorption spectra of the copper metal and its salts are shown in figure 4.1-4.6 (a). The normalization process has already been described in previous chapter of this thesis. Figures 4.1-4.6 (b) shows that the normalized absorption spectra with the pre-edge along zero, an edge step of one and the post-edge region oscillating around one for copper metal and copper salts.

[131] Joshi S. K., Sharma P. K., Shrivastava B. D., Mishra A. and Pandeya K. B., 2006, Indian J. Chemistry, **45A**, 1994.
Shrivasatava B. D., Mishra A., Joshi S. K. and Mandloi S. N., 1992, Ind. J. Chem., **31A**, 929.
Joshi S K, 1986, *Ph.D. Thesis*, Vikram University, Ujjain.
Agrawal B. K., Bhargava C.B. and Vishnoi A.N., 1976, J. Phys. Chem. Solids, **37**, 725.

4.3.1 The absorption edge

Figures 4.1-4.6 (c) indicating the positions of the absorption edge K and principal absorption maximum A in the region -30 > E > 50 eV of all copper salts, in XAFS spectra. The values of E_K for the K-absorption edge of copper metal and its salts studied are given in table 4.3. These have been determined as the energies of the first peak in the derivative spectra.

4.3.2 Position of the edge

In the region 30 > E > 50 eV, figures 4.1-4.6 (d) shows that the first derivative of absorption spectra indicating the position of the absorption edges K and principal absorption maxima A. The K- absorption edge (E_k) described by the first peak i.e., the position of first inflection point in the derivative spectra. The position where the derivative is zero, gives the position of principal absorption maxima (E_A). The results of the energies of the K-absorption edge (E_k) and the energies of principal absorption maximum A (E_A) of copper in metal and its salts are presented in table 4.3.

Figures 4.1-4.6 (e) shows that the EXAFS spectra converted into k space. The maxima and minima of the spectra for different values of k have been labelled with the conventional Latin and Greek alphabets respectively. The values of energy E and wave vector k corresponding to these maxima and minima have been given in table 4.4 for copper metal and copper salts.

4.3.3 Chemical shift

The K-absorption edge of copper has been found to be shifted towards the high energy side in all the complexes, as compared to the K-absorption edge in the copper metal. The shifts of the K-absorption edge of copper in the complexes with respect to that of copper metal have been determined according to the eqn. **$\Delta E_K = E_K$ (complex) - E_K (metal).** The chemical shifts (in eV) of the K-absorption edge of copper in the complexes are given in table 4.2. For computing the chemical shift the value of E_K (Cu metal) has been taken as 8979.27 eV. The order of the chemical shifts as indicated by their values from table 4.3 has been found to be as follows:

$CuCl_2.2H_2O < CuSO_4.5H_2O < CuBr2 < Cu(CH_3COO)_2.H_2O < Cu(NO_3)_2.3H_2O$

The compounds having copper in oxidation state in +1 show chemical shifts less than 5 eV while those having copper in oxidation state in +2 show chemical shifts more than 5 eV[132]. In table 4.3, all the salts have the values of chemical shifts between 6.57-10.80 eV copper salts. Hence, on the basis of values of the chemical shifts, all the salts are found to have copper in oxidation state +2.

As is well known, the chemical shift reflects the ionic character of the complex, more the chemical shift, more the ionic character. As the salt $Cu(NO_3)_2.3H_2O$ is showing highest chemical shift among all the salts, hence, it should have the maximum ionic character amongst the studied complexes.

4.3.4 Effective nuclear charge (ENC)

Following Gianturco et al.[133], Gupta and Nigam[134] and Nigam and Gupta[135] have outlined the method of determining the effective nuclear charge on ions from the measurement of the chemical shifts. The binding energy of an electron such as a K electron is defined as the energy required to eject the electron completely from the atom. This is equal to the difference in energy of the atom before and after ionization. If it is assumed that removal of the electron does not change the potential inside the atom appreciably, which is only true when the time of removal of the electron is short enough compared to the relaxation time of the orbit, it can be assumed that spin orbital's of the outer electrons remain unchanged during the ionization process. In this case the binding energy equals one electron eigenvalue [136] with a reversed sign.

If the binding energies of K electron of copper in different oxidation states are determined, one can find from the difference in binding energies of the neutral atom and the ionized atom, the so called theoretical shifts in the X-ray absorption edge. In the present work, the values of binding energies have been determined from the tables of Clementi and Roetti[137] using Koopman's (1934) theorem. The values of these binding energies and the theoretical shifts for copper are given in table 4.6.

---

[132] Kau L. S., Spira-Solomon D. J., Penner-Hahn J. E., Hodgson K. O., and Solomon E. I., 1987, J. Am. Chem. Soc., **109**, 6433.
[133] Gianturco F. A. and Coulson C. A., 1968, Mol. Phys., **14**, 223.
[134] Gupta M. K. and Nigam A. K., 1972(a), J. Phys. F, **2**, 1174.
Gupta M. K. and Nigam A. K., 1972(b), J. Phys. B, **5**, 1790.
[135] Nigam A. K. and Gupta M. K., 1973, J. Phys., F **3**, 1251.
Nigam A. K. and Gupta M. K., 1974, J. Phys., F **4**, 1084.
[136] Koopmans T., 1934, Physica, **1**, 104.
[137] Clementi E. and Roetti C., 1974, Atomic data and Nuclear data tables, **14**, 177.
Koopmans T., 1934, Physica, **1**, 104.

The theoretical shifts are plotted against the oxidation number. Such a graph for copper atom is shown in fig. 4.9. This graph has been obtained by fitting a third order polynomial to the points. The polynomial and the parameters are given in table 4.7. From this graph, the effective nuclear charge on copper salts has been determined and the results have been presented in table 4.3.

4.3.5 Principal absorption maximum

The principal absorption maximum A with respect to the respective K-absorption edge of all copper complexes are also given in table 4.3. It has been shown that the value of E_A of complexes is shifted towards the higher energy side with respect to copper metal. The reason for the shift of the principal absorption maximum to the higher energy side has already been discussed in previous chapter.

For the Salts mentioned in table 4.2, the energy range of chemical shift in copper salts is between 6.57-10.80 eV while the range for shift of principal absorption maximum is between 4.54-5.03 eV. Hence, on the basis of the shift of the principal absorption maximum also it can be inferred that copper is in +2 oxidation state in these copper salts. The order of shift of the principal absorption maximum in the copper salts is as follows:

$CuCl_2.2H_2O > CuSO_4.5H_2O >$CuBr2$> Cu(CH_3COO)_2.H_2O > Cu(NO_3)_2.3H_2O$

4.3.6 Edge-width

In table 4.3, the values of the edge-width (E_A-E_K) have been reported. The edge-width data for the copper salts is as follows:

$CuCl_2.2H_2O > CuSO_4.5H_2O >$CuBr2$> Cu(CH_3COO)_2.H_2O > Cu(NO_3)_2.3H_2O$

The order of the edge-width is in the reverse order of chemical shift of the complexes. The reverse order represents that the edge-width is inversely proportional to ionic character for this series. The edge-width of the K-absorption edges increase with the increase in covalent character of the bonds provided other factors like molecular

geometry etc. remain the same[138]. In the present work, edge-width of copper salts is observed to vary from 8.29-13.02.

4.3.7 Determination of bond lengths

4.3.7.1 (i) By graphical methods from EXAFS spectra

The EXAFS appearing on high energy side of the K-absorption edge have been recorded in all the copper complexes. Following the principal absorption maxima, there are distinct EXAFS features, extending up to 300 eV on the high energy side of the K-absorption edge. The K-absorption discontinuity along with fine structure for all the complexes are shown in figures 4.1-4.6 (a).

In the XAFS spectra, the inflection point on the K-absorption edge is taken as the reference point for the measurement of the extended fine structure. The positions of the EXAFS maxima and minima in eV and their corresponding values of k in $Å^{-1}$ are given in table 4.4.

The Fourier transformation technique can be used for determination of the bond lengths. The magnitudes of Fourier transform of copper metal and copper salts are shown in figures 4.1-4.6 (f) respectively and the calculated bond lengths have been shown in table 4.5. This bond length also known as phase uncorrected bond length, i.e., R_1-α_1.

The bond length can also be determined from EXAFS data by three graphical methods i.e., Levy's, Lytle's and Lytle, Sayers and Stern's (L.S.S.) methods. These methods are briefly mentioned below. Infect, before the Fourier transformation technique was formulated, the bond length used to be extracted from the EXAFS data by these three methods. We have used all the three methods for determination of bond lengths in copper salts studised in the present chapter. The bond lengths determined for the copper salts with the help of three methods are given in table 4.5.

4.3.7.1.1 (a) Levy's method[139]

It is simple method of determining bond length, according to it the bond lengths are calculated by using the eq.

$$\mathbf{R_1 = [151/\Delta E]^{1/2}\ Å}$$

[138] Kumar A., Nigam A. N. and Shrivastava B. D., 1981, X-ray Spectrom., **10**, 25
[139] Levy R. M., 1965, J. Chem. Phys., **43**, 1846.

Where ΔE is the difference of the energies of the EXAFS maximum B and minimum β and R_1 is the radius of the first coordination sphere. The positions of B and β are given in table 4.4 for the salts. The bond lengths thus determined are given in table 4.5.

4.3.7.1.2 (b) Lytle's method[140]

The energy values (E) of the EXAFS maxima, given in table 4.2, are plotted against the Q values given by Lytle, i.e., Q = 2.04, 6.0, 12.0, and 20.0. The (E, Q) plots have been found to be linear and are given in figures 4.7.

The slopes M of the E versus Q plots have been used to evaluate the radius R_s of equivalent polyhedron, by using the relation:

$$\mathbf{R_s = [37.60 / M]^{1/2}}$$

The values of R_s calculated with the help of this method are reported in table 4.5 for all the salts.

4.3.7.1.3 (c) L.S.S. method [141]

The values of the wave vector k ($Å^{-1}$) for EXAFS maxima (n = 0, 2, 4....) and minima (n =1, 3, 5....), for all the copper complexes, are presented in table 4.2.

In the Lytle, Sayers and Stern's (L.S.S.) method for determination of the nearest neighbor distances, n versus k graph is plotted. The plots have been found to be linear for all the complexes and are shown in figures 4.8. The slope of n versus k plot, gives the value of $\mathbf{2(R_1 - \alpha_1) / \pi}$, where R_1 is the bond length. The values of (R_1 - α_1) thus obtained are given in table 4.5. (Lytle F. W., Sayers D. E. and Stern E. A., 1975)

4.3.7.2 (ii) By Fourier transform of EXAFS spectra

The Fourier transform of the χ(k) versus k spectra peaks at the radial distances of the neighboring atoms from the absorbing atom. However, the distance found from Fourier transform is about 0.2 Å - 0.5 Å shorter than the actual distance due to energy dependence of the phase factors in the sine function of the EXAFS. The peaks in the Fourier transform are shifted towards the origin by an amount α_j and hence the peaks

[140] Lytle F.W., 1966, Advances in X-ray Analysis, **9**,398.
[141] Lytle F. W., Sayers D. E. and Stern E. A., 1975(a), Phys. Rev. B, **11,** 4825

are at distances R_j-α_j [142]. For the first peak j=1 and hence the position of the first peak determines the distance R_1-α_1. It is important to note here that the distance R_1-α_1 should be equal to the distance found from the L.S.S. graphical method. Hence, both the L.S.S. method and the Fourier transformation method give the value R_1-α_1, i.e., both the methods give the value of bond lengths which have not been corrected for the phase shifts. We have called this distance as the phase uncorrected bond length.

The normalized spectra are shown in figures 4.1-4.6(b) are μ (E) versus E curves obtained. From these curves, χ (k) versus k curves are obtained which are given in figures 4.1-4.6 (e).The Fourier transformed spectra obtained from χ (k) versus k curves are given in figures 4.1-4.6 (f). The position of the first peak in the Fourier transform gives the value of R_1-α_1 and the values are collected in table 4.5 for all the salts.

It is seen from table 4.5 that the value of R_1-α_1 as determined from L.S.S. method and that determined from the Fourier transformation method are in good agreement with each other, i.e., both the L.S.S. method and Fourier transformation method give nearly the same value of the phase uncorrected bond length, i.e., R_1-α_1.

4.4 Conclusions

The conclusions drawn in this chapter are as follows:

- X-ray absorption spectra of copper salts at the K-edge of copper have been recorded at the recently developed EXAFS beamline set-up at the Indus-2 synchrotron source at RRCAT, Indore.

- The K- absorption edge has been found in all copper salts. The energies of K-edge (E_K), the values of chemical shifts, the principal absorption maxima (E_A) and EXAFS maxima and minima have been reported.

- The shift of the K-edge (chemical shift) has been obtained for all copper salts. All the salts have the values of chemical shifts between 6.5-10.8 eV. The salt $Cu(NO_3)_2.3H_2O$ is showing highest chemical shift, hence, it should have the maximum ionic character amongst the studied salts. The values of the chemical shifts suggest that copper is in oxidation state +2 in all of the salts.

[142] Stern E. A., Sayers D. E. and Lytle F. W., 1975, Phys. Rev. B, **11**, 4836.

- The values of shift of the principal absorption maximum have been obtained for copper salts. The order of shift of principal absorption maximum for all the salts is in reverse order of the chemical shift. The reverse order represents that the shift of the principal absorption maximum is inversely proportional to ionic character for the salts. The salt $CuCl2.2H_2O$ is showing highest values of shift of principal absorption maxima.

- The edge-width has also been studied for all the salts. The order of the edge-width is in the reverse order of chemical shift of the salts. The reverse order represents that the edge-width is inversely proportional to ionic character for this series.

- From the positions of the EXAFS maxima and minima, the bond lengths in the salts have been determined by three different methods viz. Levy's, Lytle's and Lytle, Sayers and Stern's (L.S.S.) methods.

- The normalized spectra, i.e., μ (E) versus E curves have been obtained. From these curves, $\chi(k)$ versus k curves have been obtained, which have then been Fourier transformed using the software Athena. From the Fourier transforms of the EXAFS spectra the bond lengths have been determined.

- It has been observed that the value of the phase uncorrected bond length, i.e., $R_1-\alpha_1$ as determined from L.S.S. method and that determined from the Fourier transformation method are in good agreement with each other, i.e., both the L.S.S. method and Fourier transformation method give nearly the same value of the phase uncorrected bond length.

Table 4.2 Copper Salts and molecular formula.		
S. No.	**Salt**	**Molecular Formulae**
1.	**Copper Chloride**	**$CuCl_2.2H_2O$**
2.	**Copper Sulphate**	**$CuSO_4.5H_2O$**
3.	**Copper Bromide**	**$CuBr_2$**
4.	**Copper Acetate**	**$Cu(CH_3COO)_2.H_2O$**
5.	**Copper Nitrate**	**$Cu(NO_3)_2.3H_{2O}$**

Table 4.3 XANES data for the K-absorption edge of copper (II) salts.

Complex	E_K (eV)	E_A (eV)	Chemical shift $\Delta E_K = (E_{complex} - E_{metal})$ (eV)	ENC	Shift of the principal absorption maximum (eV)	Edge-width (E_A-E_K) (eV)
Cu metal	**8980.5**	**8995.0**	**-**	**-**	**-**	**14.56**
$CuCl_2.2H_2O$	**8987.0**	**9000.0**	**6.57**	**.72**	**5.032**	**13.027**
$CuSO_4.5H_2O$	**8987.4**	**8999.9**	**6.96**	**.73**	**4.923**	**10.522**
$CuBr_2$	**8988.2**	**8999.65**	**7.79**	**.83**	**4.593**	**11.357**
$Cu(CH_3COO)_2.H_2O$	**8989.5**	**8999.65**	**9.07**	**.89**	**4.592**	**10.076**
$Cu(NO_3)_2.3H_{2O}$	**8991.3**	**8999.60**	**10.80**	**1.1**	**4.54**	**8.299**

Table 4.4 Values of energy E and wave vector k

Energy E (eV) and wave vector k ($Å^{-1}$) for EXAFS maxima and minima at the K-absorption edge of copper Salts and their corresponding values of n, energy level Q.

Structure	n	Q	$CuCl_2.2H_2O$		$CuSO_4.5H_2O$		$CuBr_2$		$Cu(CH_3COO)_2.H_2O$		$Cu(NO_3)_2.3H_2O$	
			E (eV)	k ($Å^{-1}$)	E (eV)	k ($Å^{-1}$)	E (eV)	k ($Å^{-1}$)	E (eV)	k ($Å^{-1}$)	E (eV)	k ($Å^{-1}$)
A	0	2.04	12.5	1.82	10.1	1.64	15.5	2.02	8.78	1.52	11.77	1.76
α	1	-	42.1	3.33	40.40	3.26	39.6	3.23	33.53	2.97	33.53	2.97
B	2	6.04	59.5	3.95	59.62	3.96	58.1	3.91	54.90	3.80	54.61	3.79
β	3	-	123.5	5.77	123.2	5.71	68.6	4.25	123.5	5.77	95.05	5.0
C	4	12.00	158.1	6.45	141.9	6.11	92.4	4.93	153.3	6.35	148.5	6.25
γ	5	-	243.3	8.00	238.5	7.92	126.1	5.76	243.9	8.03	239.7	7.94
D	6	20.00	286.4	8.68	282.5	8.62	155.7	6.40	272.7	8.47	278.6	8.56

Table 4.5 Values of first shell bond lengths (in Å)

calculated from Levy's, Lytle's, L.S.S. and Fourier transform methods for copper (II) Salts

S. No.	Complex	Phase corrected		Phase uncorrected	
		Levy's method R_1	Lytle's method R_s	L.S.S. method R_1-α_1	F.T. method R
1.	$CuCl_2.2H_2O$	1.53	1.56	1.34	1.37
2.	$CuSO_4.5H_2O$	1.48	1.57	1.33	1.39
3.	$CuBr_2$	2.78	2.23	2.24	2.22
5.	$Cu(CH_3COO)_2.H_2O$	1.48	1.58	1.30	1.22
6.	$Cu(NO_3)_2.3H_{2O}$	1.93	1.57	1.28	1.41

Table 4.6 Binding energies of 1s electrons of copper atom in different oxidation states.				
Oxidation state	**Electronic configuration**	**B.E. of 1s electrons (au)**	**Shift in B.E. (in au)**	**Shift in B.E. (in eV)**
0	$3d^{10}\ 4s^{1}$	**328.79173**	**-**	**-**
+1	$3d^{10}\ 4s^{0}$	**329.10745**	**0.3157**	**8.59**
+2	$3d^{9}\ 4s^{0}$	**329.76836**	**0.9766**	**26.57**
+3	$3d^{8}\ 4s^{0}$	**330.55359**	**1.7618**	**47.94**
+4	$3d^{7}\ 4s^{0}$	**331.45117**	**2.6594**	**72.37**
+5	$3d^{6}\ 4s^{0}$	**332.48020**	**3.6884**	**100.37**
+6	$3d^{5}\ 4s^{0}$	**333.59556**	**4.8038**	**130.72**

Note - 1 au = 2ry = 27.2116eV

The above values have been fitted to the polynomial curve.

$$y = A + B_1x + B_2x^2 + B_3x^3$$

Table 4.7 The parameters and polynomials are given below:

Parameter	Value	Error
A	**-0.40262**	**0.84812**
B_1	**6.59889**	**1.33947**
B_2	**3.67952**	**0.54746**
B_3	**-3.44467**	**0.05989**

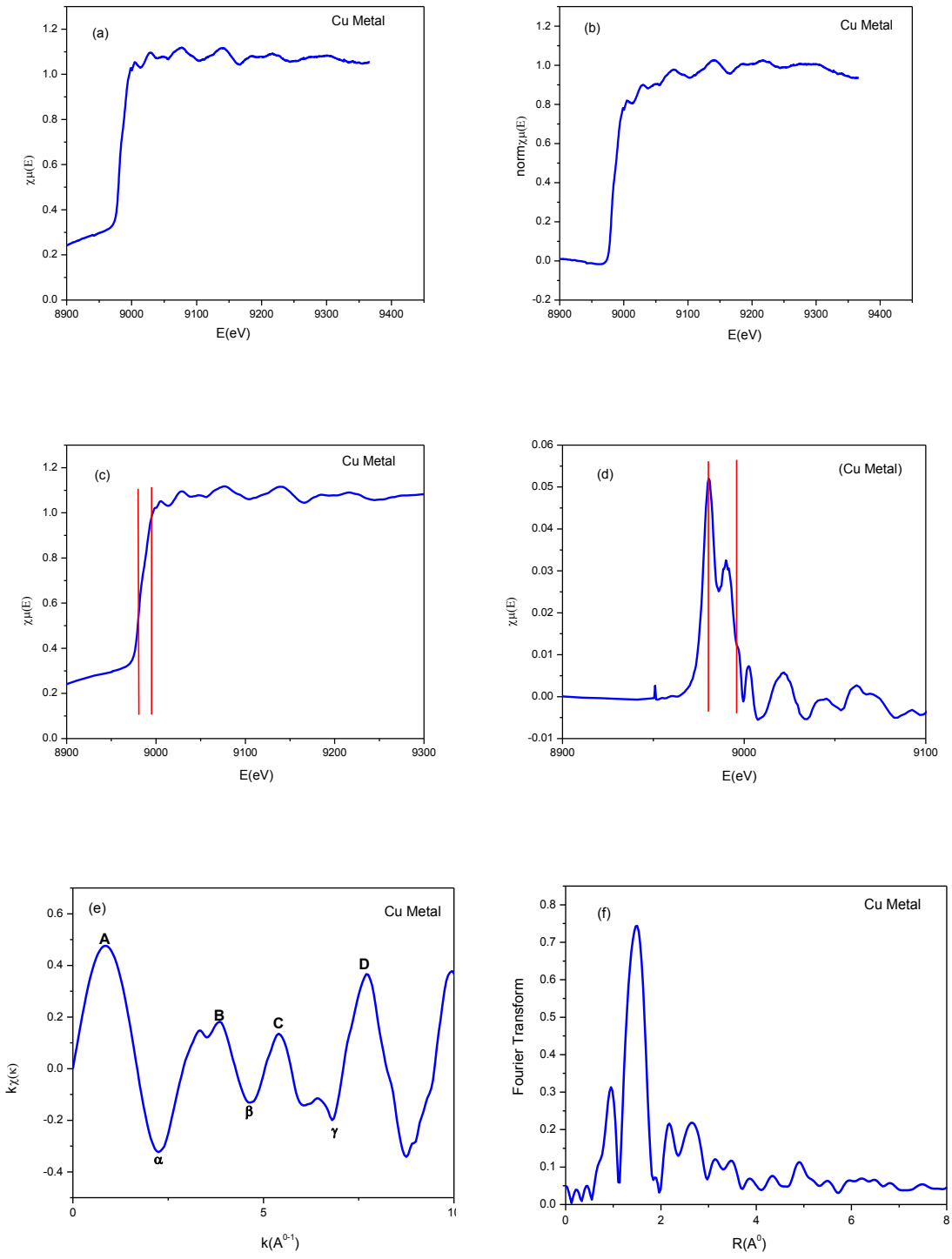

Figure 4-1 XAFS data analysis curves for copper metal.

(a) Raw absorption versus photoelectron energy (b) The normalized absorption spectrum (c) XAFS spectrum and (d) Derivative of XAFS spectrum for copper metal indicating position of absorption edge K and principal absorption maxima A. (e) χ(k) versus k curve and (f) Magnitude of Fourier transform of the χ(k) versus k curve.

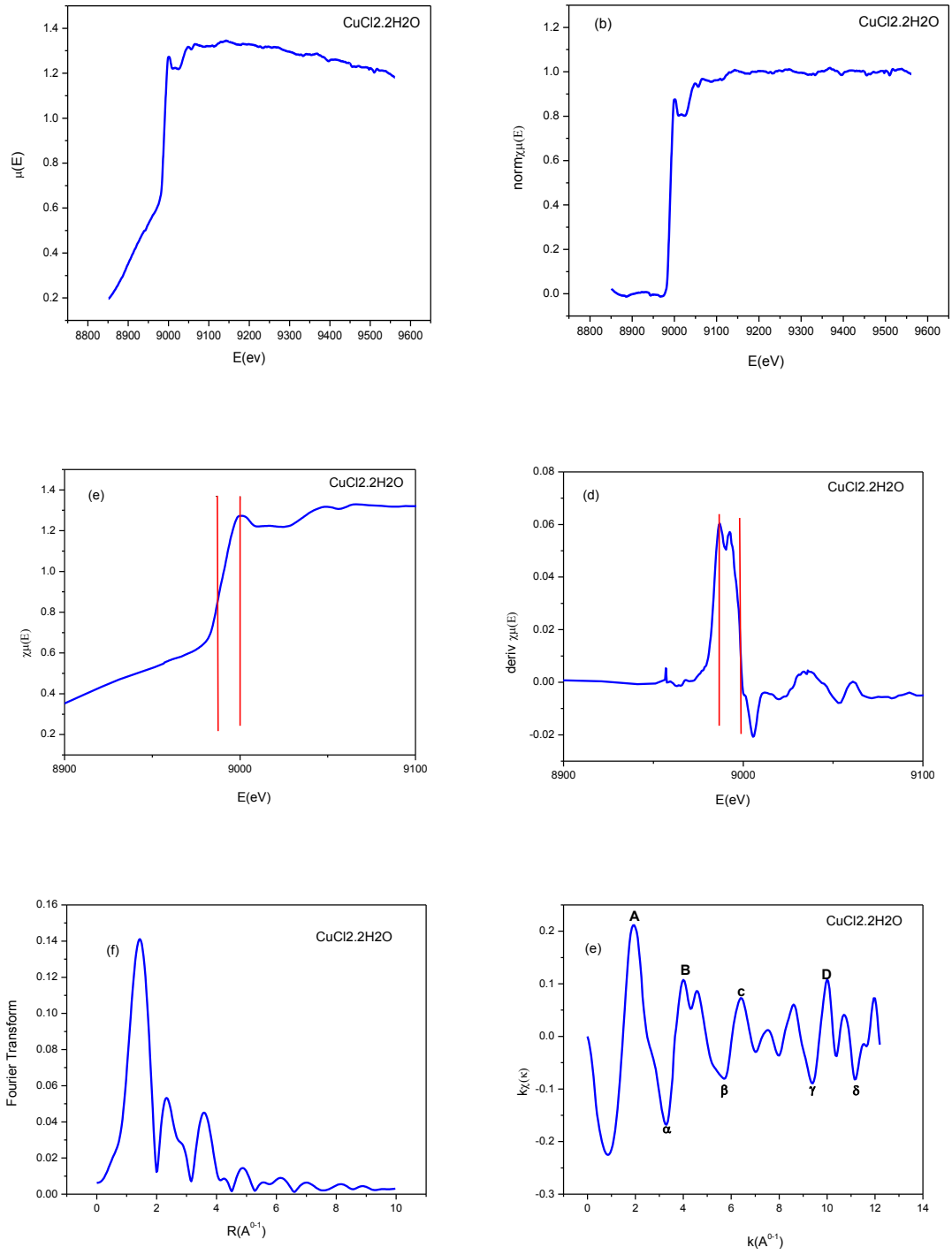

Figure 4-2 XAFS data analysis curves for $CuCl2.2H_2O$.

(a) Raw absorption versus photoelectron energy (b) The normalized absorption spectrum (c) XAFS spectrum and (d) Derivative of XAFS spectrum for copper metal indicating position of absorption edge K and principal absorption maxima A. (e) χ(k) versus k curve and (f) Magnitude of Fourier transform of the χ(k) versus k curve.

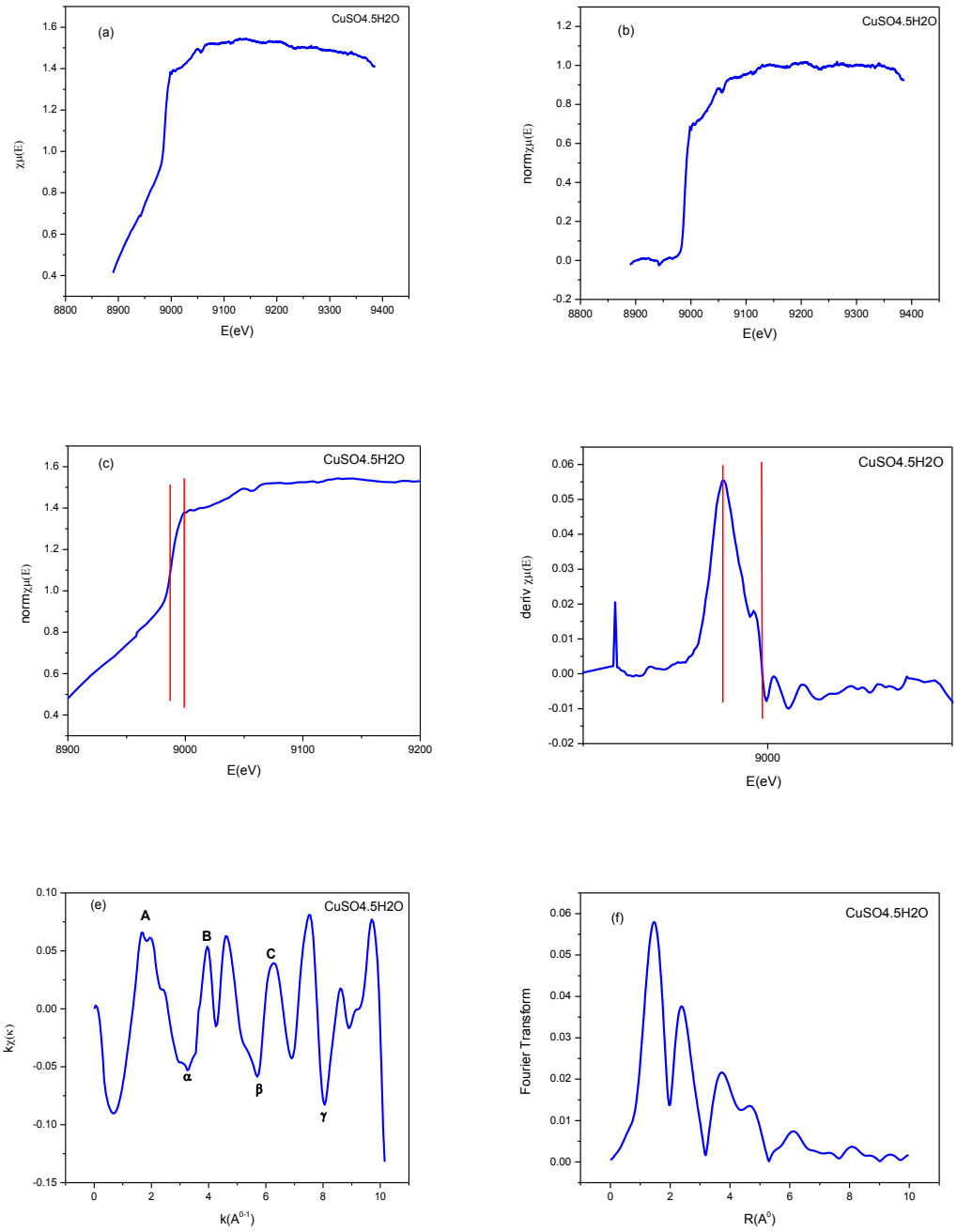

Figure 4-3 XAFS data analysis curves for $CuSO_4.5H_2O$.

(a) Raw absorption versus photoelectron energy (b) The normalized absorption spectrum (c) XAFS spectrum and (d) Derivative of XAFS spectrum for copper metal indicating position of absorption edge K and principal absorption maxima A. (e) χ(k) versus k curve and (f) Magnitude of Fourier transform of the χ(k) versus k curve.

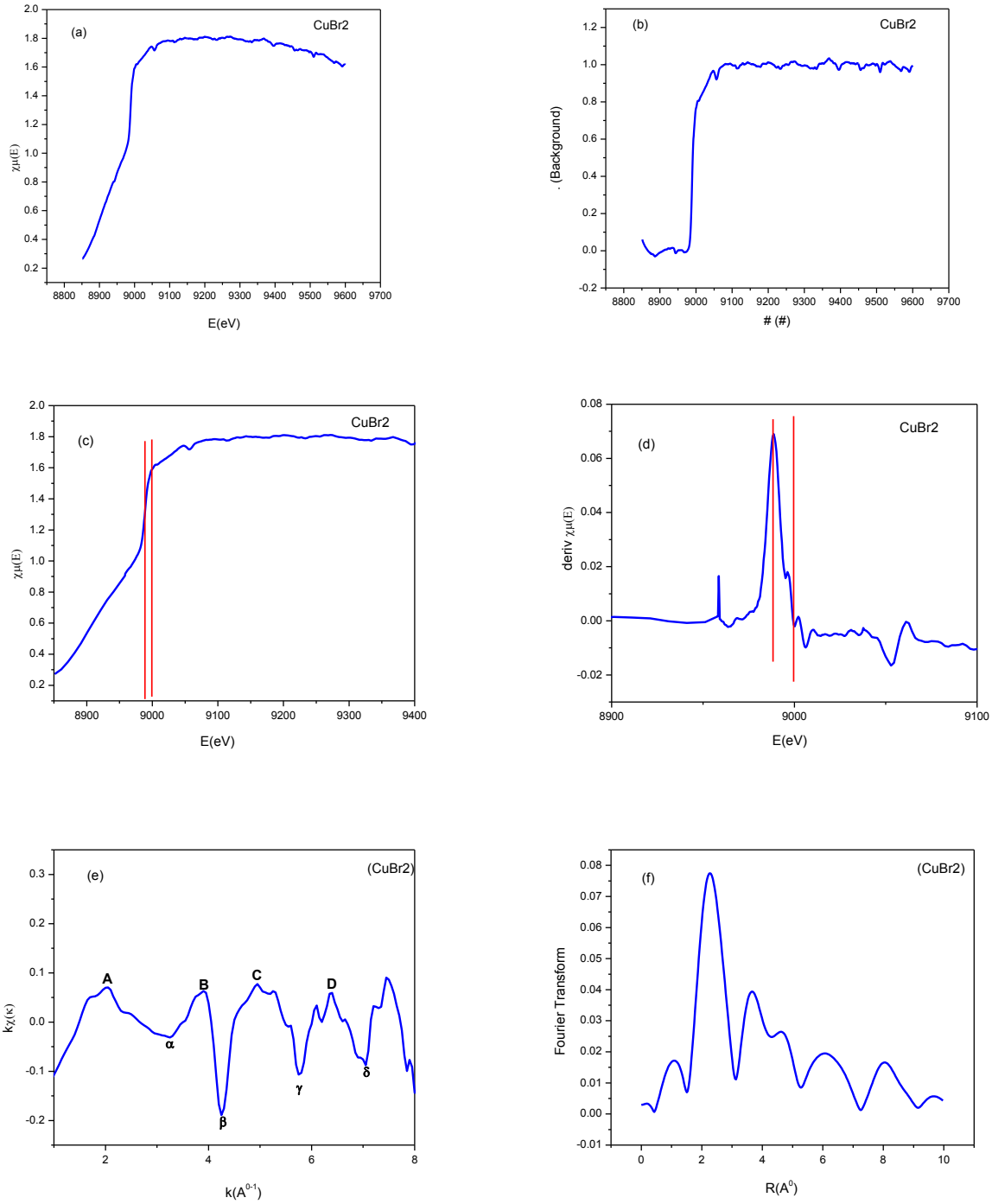

Figure 4-4 XAFS data analysis curves for $CuBr_2$.

(a) Raw absorption versus photoelectron energy (b) The normalized absorption spectrum (c) XAFS spectrum and (d) Derivative of XAFS spectrum for copper metal indicating position of absorption edge K and principal absorption maxima A. (e) χ(k) versus k curve and (f) Magnitude of Fourier transform of the χ(k) versus k curve.

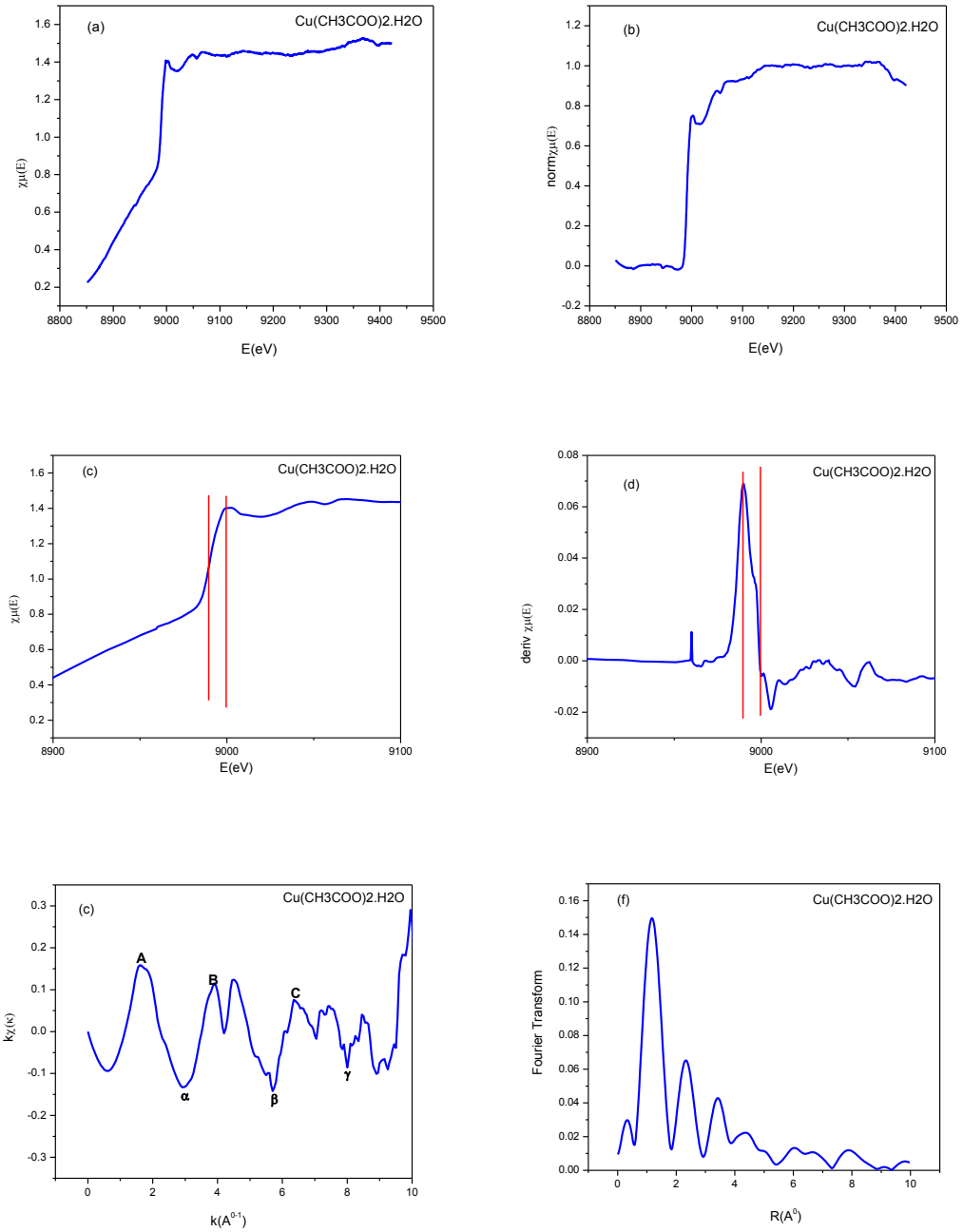

Figure 4-5 XAFS data analysis curves for Cu $(CH_3COO)_2.H_2O$

(a) Raw absorption versus photoelectron energy (b) The normalized absorption spectrum (c) XAFS spectrum and (d) Derivative of XAFS spectrum for copper metal indicating position of absorption edge K and principal absorption maxima A. (e) χ(k) versus k curve and (f) Magnitude of Fourier transform of the χ(k) versus k curve.

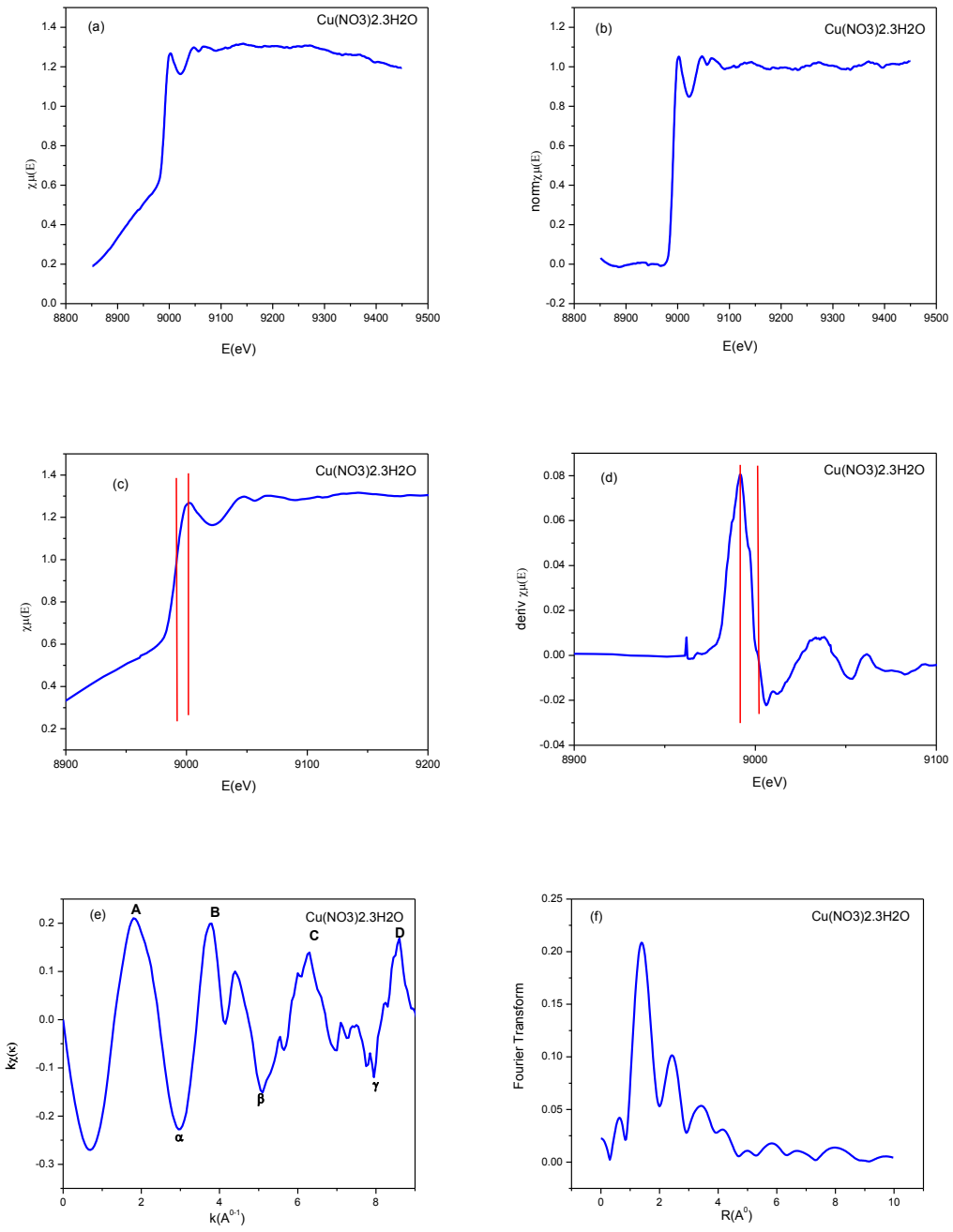

Figure 4-6 XAFS data analysis curves for $Cu(NO_3)_2.3H_{2O}$

(a) Raw absorption versus photoelectron energy (b) The normalized absorption spectrum (c) XAFS spectrum and (d) Derivative of XAFS spectrum for copper metal indicating position of absorption edge K and principal absorption maxima A. (e) χ(k) versus k curve and (f) Magnitude of Fourier transform of the χ(k) versus k curve.

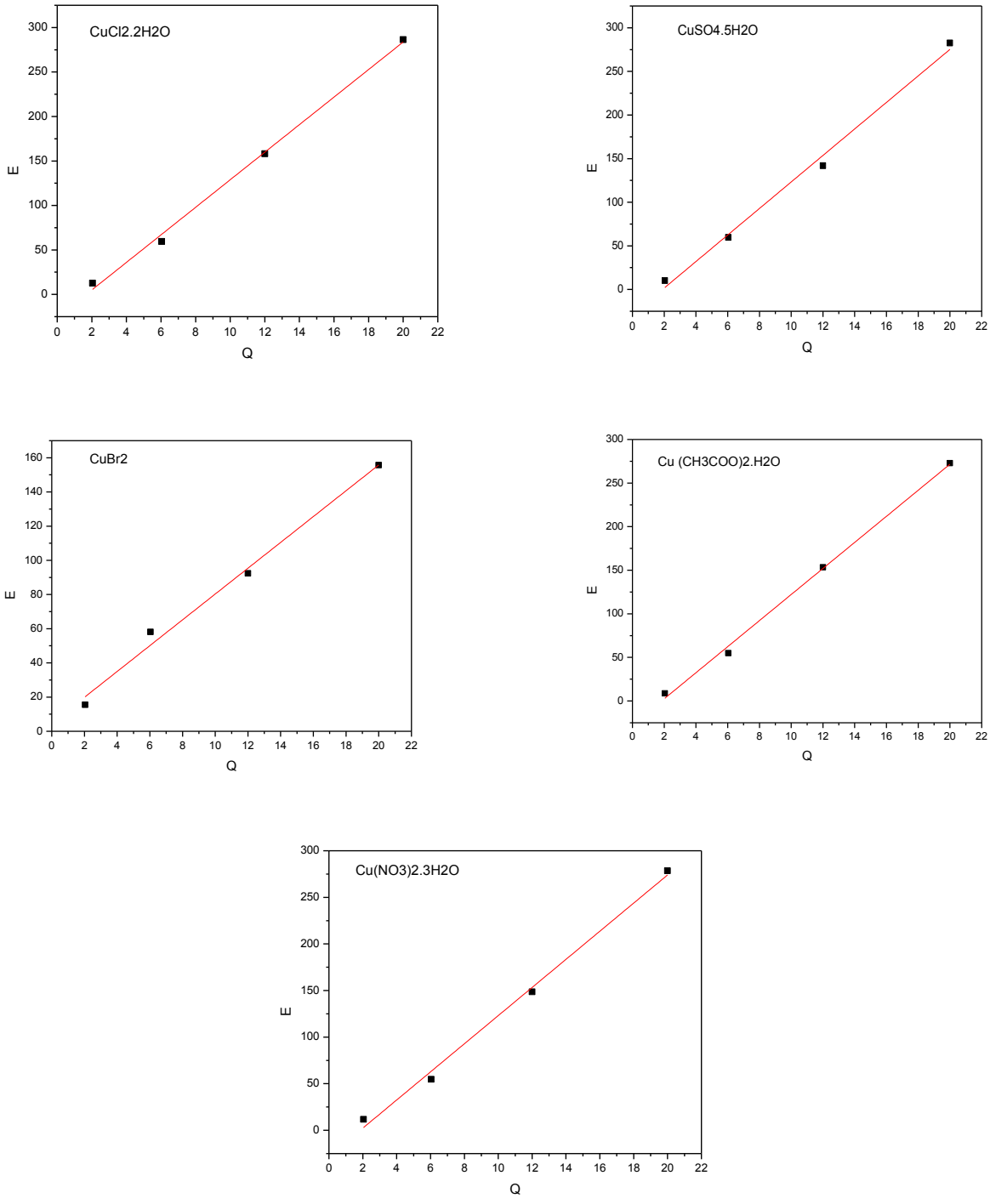

Figure 4-7 E versus Q curves for the copper salts

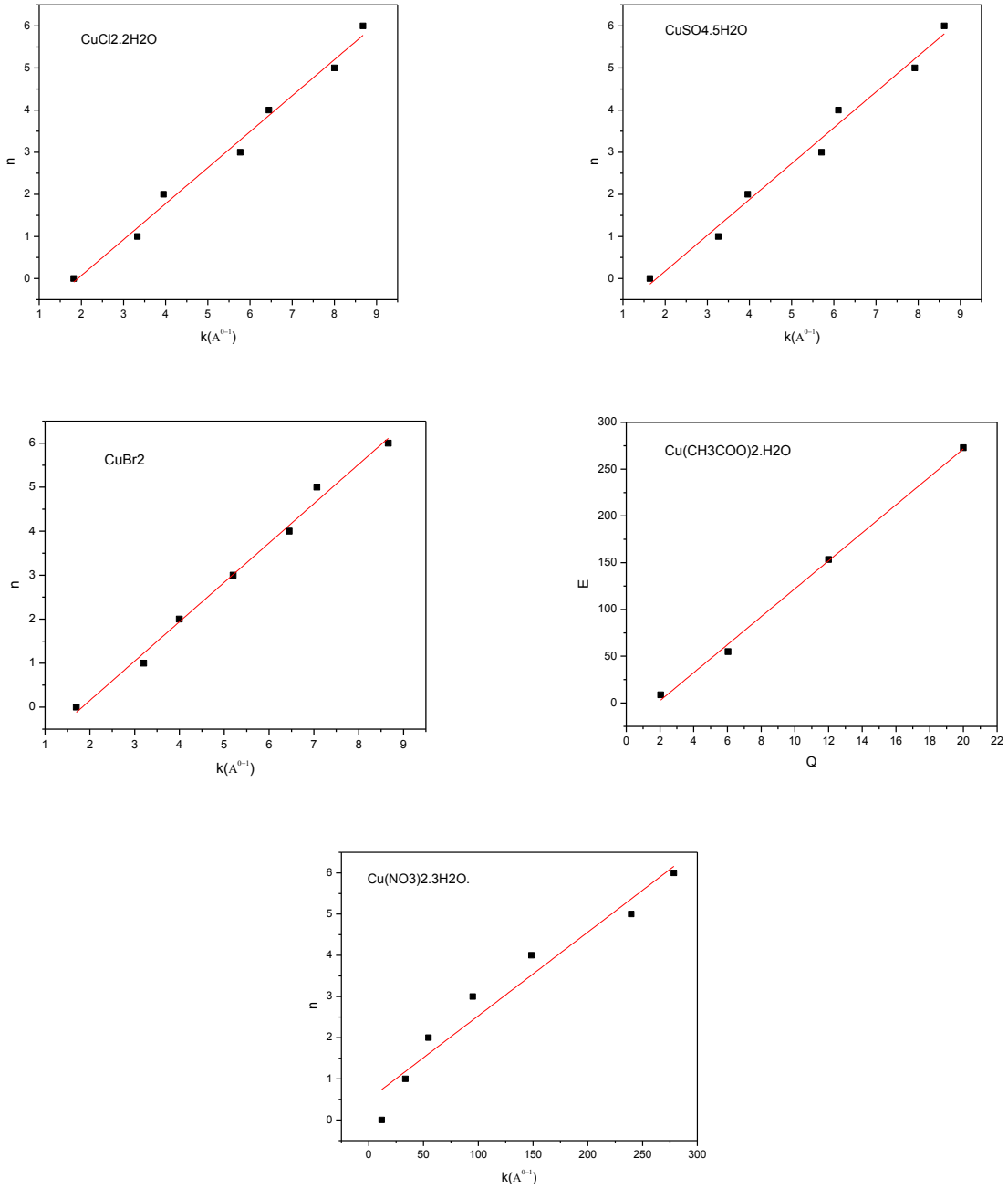

Figure 4-8 n versus k curves for the copper Salts

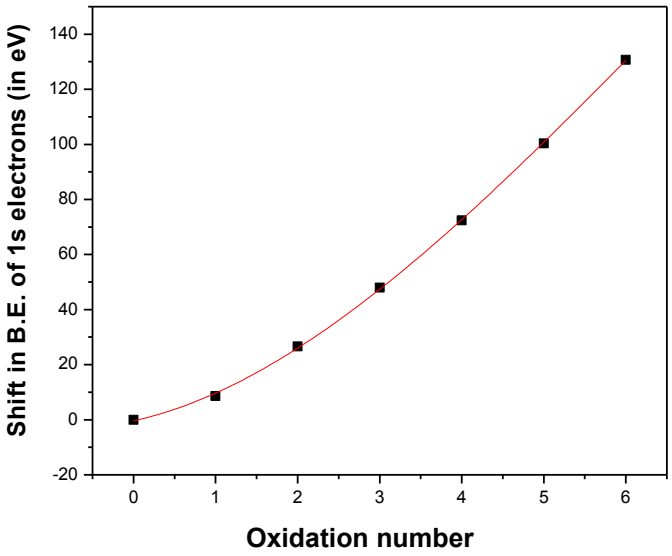

Figure 4-9 Plot of oxidation number versus shift in B.E. of 1s electrons as given in table 4.5.

***